Dielectric response of a quasi-one-dimensional electron system

1990 J. Phys.: Condens. Matter 2 9381

(http://iopscience.iop.org/0953-8984/2/47/013)

J. Phys.: Condens. Matter 2 (1990) 9381–9397. Printed in the UK

Dielectric response of a quasi-one-dimensional electron system

G Y Hu and R F O'Connell

Department of Physics and Astronomy, Louisiana State University, Baton Rouge, LA 70803-4001, USA

Received 27 April 1990, in final form 17 July 1990

Abstract. The dielectric response of a quasi-one-dimensional electron system is studied by including fluctuation effects (in the polarizability) and by using a recently derived analytic form for the electron–electron interactions. General forms for the polarizability matrices both for the intra- and inter-subband cases are presented. The generalized polarizability is analytic over the whole region of the wavevectors and rigorously retains the number neutrality. Various differences between the intra- and inter-subband cases for the polarizability and the dielectric matrix function are studied. The theory is used to study impurity screening and plasmon excitations in the presence of multi-subbands. We show that the screened impurity potential of a quasi-one-dimensional electron system is a well defined quantity and, in contrast to its two- and three-dimensional counterparts, it is finite at the origin and has stronger Friedel oscillations. An explanation is given for the experimental results of Hansen *et al* concerning the relationship between the inter-subband plasmon frequencies and the electron densities.

1. Introduction

Recently, there has been widespread interest in studying the physics of semiconductor quantum wires (which have a width of the order of 10^3 Å, comparable with the Fermi wavelength), where many novel effects with exciting possibilities for device applications have been detected [1–9]. The electrons in these quantum wires are free to move in one direction (say, along the x-axis) and are restricted in another (the y-axis) direction in some kind of quantized motion. Such semiconductor quantum wires are referred to as quasi-one-dimensional (Q1D) systems. With a view toward understanding more about these Q1D systems, we consider one of the most important properties namely the dielectric response function.

A number of papers [3–9] have been published in which the dielectric function of Q1D systems has been studied. These studies show that the main difficulty in studying the dielectric response of Q1D systems is that the $T = 0$ free-electron polarizability diverges at the wavevector $q = 2k_F$, where k_F is the Fermi wavevector [3, 4]. In addition, the form of the Q1D Coulomb potential depends heavily on the confinement model used in the calculation and is generally evaluated numerically both for the intra- and inter-subband cases. At $T = 0$, in order to obtain a better behaved Q1D polarizability, various attempts have been made to go beyond the free electron approximation by including other effects:

0953-8984/90/479381+17$03.50

(1) the electron–electron interaction in the Hubbard–Singwi approach [3]; and
(2) the electron–impurity effect in the relaxation time approximation [5, 6].

The Hubbard–Singwi approach does not directly address the $q = 2k_F$ divergence, while the relaxation time approximation in modifying the free electron polarizability is known to be complicated by virtue of having to retain the number neutrality of the electrons, i.e. the screening charge equals the impurity charge, a required property for any form of polarizability [10, 11].

In this paper, we present another form for the Q1D polarizability beyond the free electron approximation. The new generalized Q1D polarizability is analytic at $q = 2k_F$ and is rigorous in the sense that it retains the number neutrality requirement in a natural way. It is obtained by including the physical effects of fluctuations in the polarizability which arise from the electron–electron, electron–phonon and the electron–impurity interactions (in a manner similar to our previous generalization of the Lindhard function in three dimensions [11] and the Stern function in two dimensions [12]). In addition to the study of the Q1D polarizability, we also apply a recently derived analytical form of the Q1D electron–electron interaction [13], which serves to make the analytical study of the dielectric response function possible.

To clarify the terminology, here we mention that the term 'Q1D system' is also widely used [14] for the study of metal filaments and conducting compounds, which have a width of the order of several atomic units, i.e. electrons in a Q1D lattice. There, the main interest appears to be the many novel electronic behaviours related to the Q1D lattice such as the Peierls instability and charge density wave, and other phase-coherent problems such as superconductivity and weak localization. There exists a vast literature [14] concerning the dielectric response of the system under the influence of some of these physical processes, and very often the Tomonaga–Luttinger model and the bosonization method are used. The semiconductor quantum wires, which are the subject of this paper, are different from the metal filaments and conducting compounds in that the Q1D electrons in the semiconductor quantum wires are contained in a bulk-like lattice (negligible Peierls instability). In addition, the real sample used in the experiments is usually composed of many parallel semiconductor quantum wires (e.g. there are 10^4 wires in the sample used in [1]) and the quantum interference effect is assumed to be negligible due to statistical averaging. In other words, we are concerned only with the normal state response behaviour of the Q1D electrons based on the usual Landau–Fermi liquid picture (which is different from the Tomonaga–Luttinger model [14]). For these reasons, no attempt will be made to relate the main results of this paper to the dielectric response of the metal filaments or conducting compounds.

In section 2, we describe the model we used and we present a formal discussion of our results for the Q1D Coulomb matrix elements, the polarization function and the dielectric response function. In section 3, we evaluate the Q1D polarizability and obtain a general analytical form, which includes both the intra- and inter-subband cases. In section 4, we study the dielectric matrix function using the results of the previous sections. As an application, in section 5 we study the screened impurity potential and the plasmon excitations in the presence of many populated subbands. Our results are summarized and discussed in section 6.

2. Model

We consider a two-dimensional electron gas in a zero thickness xy-plane with a har-

monic confinement potential in the y-direction.

In the harmonic confinement model [13], the one electron wavefunction is

$$\psi(x,y,z) = \frac{e^{iqx}}{\sqrt{L}}\xi_n(y)\delta(z) \tag{2.1}$$

where the delta-function indicates that we neglect the z-direction motion of the electrons

$$\xi_n(y) = \left(\frac{1}{2^n n!\sqrt{\pi}b}\right)^{1/2} e^{-y^2/2b^2} H_n\left(\frac{y}{b}\right) \tag{2.2}$$

$H_n(x)$ is the Hermite polynomial, $b = (\hbar/m^*\omega_0)^{1/2}$, m^* is the electron effective mass and ω_0 is the characteristic frequency of the harmonic potential.

Our model Hamiltonian for this Q1D system is written in the centre-of-mass and relative electron coordinates, in a manner similar to the one we used in [15], as

$$H = H_C + H_B + H_I \tag{2.3a}$$

$$H_C = \frac{P^2}{2M} - NeE\cdot R \tag{2.3b}$$

$$H_B = \sum_{nk} \varepsilon_{kn} C^+_{kn} C_{kn} + \frac{1}{2L} \sum_{\substack{kk'q \\ n_1 n_2 n_3 n_4}} V_{\{N\}}(q) C^+_{k+q,n_2} C^+_{k'-q,n_4} C_{k',n_3} C_{k,n_1} \tag{2.3c}$$

where H_C, H_B and H_I refer, respectively, to the Hamiltonians for the centre-of-mass, the heat-bath (relative electrons) and the interaction. Also $\boldsymbol{P}$ and $\boldsymbol{R}$ are the centre-of-mass momentum and position, $C^+_{kk_n}$ and C_{kk_n} are the creation and annihilation operators for relative electrons with wavevector $\boldsymbol{k} = (k, k_n)$. In addition, $V_{\{N\}}(q)$ is the Q1D Coulomb matrix having the general form [13]

$$V_{\{N\}}(q) = \begin{cases} (e^2/\kappa)E_{\{N\}}(qb) & N \text{ even} \\ 0 & N \text{ odd} \end{cases} \tag{2.4a}$$

where $N = n_1 + n_2 + n_3 + n_4$, $\{N\}$ represents $\{n_1 n_2, n_3 n_4\}$, κ is the dielectric constant of the static lattice and

$$E_{\{N\}}(qb) = \sum_{s=0}^{N/2} C_s^{\{N\}} \int_0^\infty dy \frac{e^{-y/2}}{\sqrt{y(y+b^2q^2)}} \left\{\frac{y}{y+b^2q^2}\right\}^s. \tag{2.4b}$$

Here $C_s^{\{N\}}$ are some numbers which depends on s and $\{N\}$, the general form of which are presented in appendix A of [13] and some of the values are given in table 1 of [13]. For later use we mention that, for a two subband system, there are only four kinds of non-zero values for the Coulomb matrix (2.4), which have the analytic forms

$$V_{00,00}(q) = \frac{e^2}{\kappa} e^{b^2q^2/4} K_0(\tfrac{1}{4}b^2q^2) \tag{2.5a}$$

$$V_{11,11}(q) = \frac{e^2}{\kappa} e^{b^2q^2/4}\{(1+\tfrac{1}{2}b^2q^2+\tfrac{1}{8}b^4q^4)K_0(\tfrac{1}{4}b^2q^2) - \tfrac{1}{4}b^2q^2(1+\tfrac{1}{2}b^2q^2)K_1(\tfrac{1}{4}b^2q^2)\} \tag{2.5b}$$

$$V_{00,11}(q) = \frac{e^2}{\kappa} e^{b^2q^2/4}\{K_0(\tfrac{1}{4}b^2q^2) + \tfrac{1}{4}b^2q^2[K_0(\tfrac{1}{4}b^2q^2) - K_1(\tfrac{1}{4}b^2q^2)]\} \tag{2.5c}$$

$$V_{01,01}(q) = \frac{e^2}{\kappa} e^{b^2q^2/4}\tfrac{1}{4}b^2q^2\{K_1(\tfrac{1}{4}b^2q^2) - K_0(\tfrac{1}{4}b^2q^2)\} \tag{2.5d}$$

where $K_n(x)$ is the nth order modified Bessel function of the second kind. The presence of H_I together with the electron–electron interaction in (2.3c) modifies the response of the electron gas. According to the generalized quantum Langevin approach, these modifications can be considered by studying the fluctuation effects, which are represented by the diffusion constant of the centre-of-mass electrons [11]

$$D = \lim_{t\to\infty} \frac{1}{2t}\langle R^2(t)\rangle. \tag{2.6}$$

When the fluctuation effect is included, one obtains the Q1D polarizability, similar to the two- and three-dimensional cases [11, 12]

$$\chi(q,\omega) = \frac{1}{WL}\sum_{k,nn'} \frac{f_k - f_{k+q}}{\hbar\omega - (\epsilon_{k+q} - \epsilon_k) + iDq^2} C_n(q_l) \tag{2.7}$$

where W is the width, L is the length of the Q1D system, f_k is the Fermi distribution function

$$q = (q, q_l) \qquad \text{and} \qquad \varepsilon_k \equiv \varepsilon_{kk_n} = \frac{\hbar^2 k^2}{2m^*} + (n + \tfrac{1}{2})\hbar\omega_0.$$

In addition $C_n(q_l)$ is a factor due to the lateral quantization. In the harmonic model, which we adopt here, it is given by

$$C_n(q_l) = \left| \int dy\, e^{-iq_l y} \xi_n^*(y)\xi_{n+l}(y) \right|^2 \tag{2.8}$$

where $\xi_n(y)$ is defined in (2.2) and $n' = n + l$.

The analytic form (2.4) of the Coulomb matrix elements and the generalized polarizability (2.7) of the Q1D system are the basic ingredients for the discussion of the dielectric response, which is the subject of the following sections.

3. Polarizability at $T = 0$

In this section we evaluate the Q1D polarizability (2.7) at $T = 0$. When $T = 0$, the Fermi distribution function is a step function $f_{kk_n} = \theta(\varepsilon_F - \varepsilon_{kk_n})$, where ε_F is the Fermi energy, and the summation over k in (2.7) can be carried out easily by using the continuum approximation $\sum_k \to L/2\pi \int dk$. After some algebra, we obtain from (2.7) the $T = 0$ polarizability with the fluctuation effects as

$$\chi(q,\omega) = \frac{1}{W}\sum_{n,n'}^{M} \chi_{nn'}(q,\omega) C_n(q_l) \tag{3.1}$$

where M denotes the top populated subband, $n, n' = n+l$ are subband indices involved in the electron response and $C_n(q_l)$ is defined by (2.8). Also, the polarization matrix element $\chi_{nn'}$ in (3.1) is obtained explicitly as

$$\chi_{nn'}(q,\omega) = -\frac{m^*}{\pi q} \ln \frac{(b_n - \nu_-(l) - i\frac{1}{2}ax)(b_{n'} + \nu_+(l) + i\frac{1}{2}ax)}{(b_n + \nu_-(l) + i\frac{1}{2}ax)(b_{n'} - \nu_+(l) - i\frac{1}{2}ax)} \tag{3.2}$$

where the spin degeneracy has been taken into account, and

$$a = 2m^*D/\hbar \qquad b_n = bk_{Fn}$$
$$k_{Fn}^2 = 2m^*(\varepsilon_F - n\hbar\omega_0)/\hbar^2 \qquad (k_{Fn} = 0, \text{ if } \epsilon_F < n\hbar\omega_0) \tag{3.3}$$

and

$$\nu_\pm(l) = \frac{y-l}{x} \pm \frac{x}{2} \qquad x = bq \qquad y = \frac{\omega}{\omega_0}. \tag{3.4}$$

The polarization matrix element (3.2) is the core of the Q1D polarizability (3.1). In the following we study (3.2) in detail for the intra- and inter-subband cases.

3.1. Intra-subband polarization matrix element

The intra-subband polarization matrix element is defined by taking $n = n'$ in (3.2). In this (3.2) reduces to

$$\chi_{nn}(x,y) = -\frac{m^*}{\pi q} \ln \frac{(b_n + \frac{1}{2}x)^2 + a^2x^2 - (y/x)^2 - 2iay}{(b_n - \frac{1}{2}x)^2 + a^2x^2 - (y/x)^2 - 2iay}. \tag{3.5}$$

When $n = 0$ and $a \to 0$, (3.5) reduces to the special case of the one subband polarizability of the Q1D non-interacting electrons

$$\chi^\circ(x,y) = -\frac{m^*}{\pi q}\left\{\ln \frac{(b_0x + \frac{1}{2}x^2)^2 - y^2}{(b_0x - \frac{1}{2}x^2)^2 - y^2} - i\pi\theta(b_0x + \tfrac{1}{2}x^2 - y)\theta(y - b_0x + \tfrac{1}{2}x^2)\right\}. \tag{3.6}$$

We note that the real part of (3.6) is divergent at $y = |b_0x \pm \frac{1}{2}x^2|$. In the work of Das Sarma and Lai, they eliminated the $2k_F$ divergence of (3.6) by including both the thermal and the impurity collisional effects. Here we have avoided the divergence problem by including the fluctuation effects represented by the parameter a. The difference is that (3.5) retains the conservation of the local electron number while incorporating the electron collisional effect into the polarization, a point first noted by Mermin in his study of the Lindhard function [10]. In addition, (3.5) has more advantages:

(i) only one parameter a is involved, which represents the inelastic electron–electron and electron–phonon interaction effects on the polarization;

(ii) analytic forms of both the real and imaginary parts of the polarizability matrix elements can be deduced directly from (3.5), which makes it very convenient for use in the study of the dielectric properties of Q1D systems.

In figure 1(*a*), we plot the static function $-\chi_{00}(q)$ of (3.5) in units of $m^*/2\pi k_F$, and we choose $a = 0.1$ and 0.01. We observe from the figure that the original $q = 2k_F$ divergence of $\chi^0(q)$ of (3.6) is eliminated because of the fluctuation effects represented by a, and the larger the value of a the broader the $q = 2k_F$ peak. When $n \neq 0$, it is easy to see that $\chi_{nn}(q)$ will have the same behaviour as χ_{00} except that now the peak is located at $q = 2k_{Fn}$. This is illustrated in figure 1(*b*), where we take $a = 0.01$ and $n = 0, 1, 2$, to plot $\chi_{nn}(q)$ in units of $m^*/2\pi k_{Fn}$. Figure 1 shows that, in general, the intra-subband polarizability matrix has the following properties:

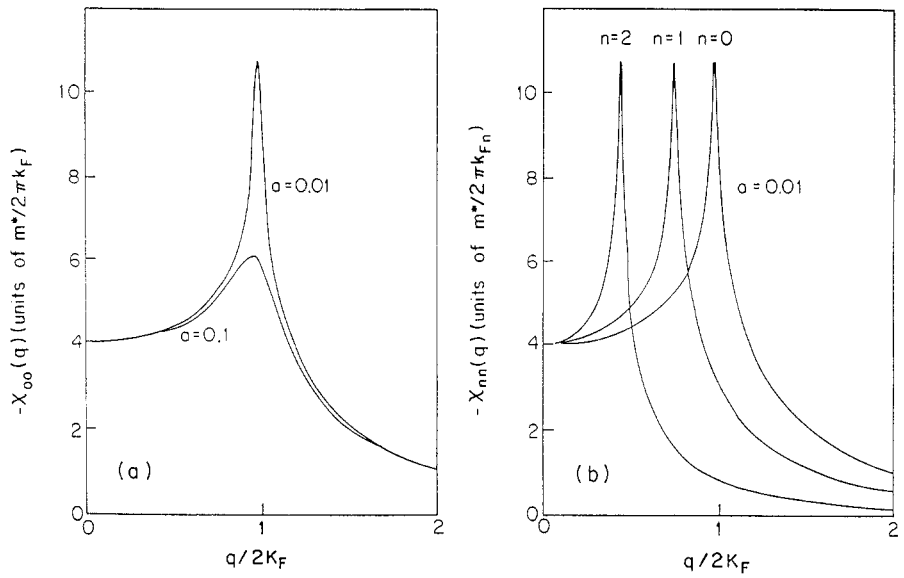

Figure 1. Static intra-subband polarization matrix elements $-\chi_{nn}(q)$ as a function of $q/2k_F$: (*a*) $n = 0$ for two broadening parameters $a = 0.1$ and 0.01; (*b*) $a = 0.01$ for three different subband indices $n = 0, 1, 2$.

(i) in the $q \to 0$ limit, it approaches a constant independent of the subband separation;

(ii) it peaks near $q = 2k_{Fn}$; and

(iii) it vanishes as q^{-2} in the $q \to \infty$ limit.

The $q \to 0$ expansion formula of the real part of (3.5) is useful for studying plasmon excitations. From (3.5) it is easy to obtain

$$\chi_{nn}(q \to 0, \omega) = \frac{2q^2 k_{Fn}}{m^* \pi \omega^2} + O(q^4). \tag{3.7}$$

3.2. Inter-subband polarization matrix element

When $n \neq n'$, (3.2) represents the inter-subband polarization matrix element. After some algebra, the real and imaginary part of (3.2) can be written respectively as

$$\mathrm{Re}\,\chi_{nn'}(x,y) = -\frac{m^*}{2\pi q} \ln \frac{[(b_n - \nu_-(l))^2 + \frac{1}{4}a^2x^2][(b_{n'} + \nu_+(l))^2 + \frac{1}{4}a^2x^2]}{[(b_n + \nu_-(l))^2 + \frac{1}{4}a^2x^2][(b_{n'} - \nu_+(l))^2 + \frac{1}{4}a^2x^2]} \tag{3.8a}$$

$$\mathrm{Im}\,\chi_{nn'}(x,y) = \frac{m^*}{\pi q}\left\{\pi[\theta(b_{n'}^2 - \nu_+^2(l) - \tfrac{1}{4}a^2x^2) - \theta(b_n^2 - \nu_-^2(l) - \tfrac{1}{4}a^2x^2)] + \tan^{-1}\frac{axb_n}{\nu_-^2(l) - b_n^2 + \frac{1}{4}a^2x^2} - \tan^{-1}\frac{axb_{n'}}{\nu_+^2(l) - b_{n'}^2 + \frac{1}{4}a^2x^2}\right\} \tag{3.8b}$$

where the arguments are defined by (3.3) and (3.4), and $\theta(x)$ is the step function.

First, it is clear that (3.8*a*) and (3.8*b*) have the following symmetry properties

$$\mathrm{Re}\,\chi_{nn'}(q,-\omega) = \mathrm{Re}\,\chi_{n'n}(q,\omega) \tag{3.9a}$$

$$\mathrm{Im}\,\chi_{nn'}(q,-\omega) = -\mathrm{Im}\,\chi_{n'n}(q,\omega). \tag{3.9b}$$

Equations (3.9*a*) and (3.9*b*) in the static limit give

$$\mathrm{Re}\,\chi_{nn'}(q) = \mathrm{Re}\,\chi_{n'n}(q) \tag{3.10a}$$

$$\mathrm{Im}\,\chi_{nn'}(q) = \mathrm{Im}\,\chi_{n'n}(q) = 0. \tag{3.10b}$$

We note that the symmetry properties (3.9*a*) and (3.9*b*) for the polarization matrix elements $\chi_{nn'}$ are the necessary conditions for the Q1D polarizability (2.7) to have $\mathrm{Re}\,\chi(q,-\omega) = \mathrm{Re}\,\chi(q,\omega)$ and $\mathrm{Im}\,\chi(q,-\omega) = -\mathrm{Im}\,\chi(q,\omega)$, which must be satisfied by any kind of response function. Also, we note that (3.10*a*) implies that in studying the static behaviour we have only to consider one of the $\chi_{nn'}(q)$ and $\chi_{n'n}(q)$. In the following, we first study the long wavelength limit behaviour of (3.8*a*) and then its static function $\chi_{nn'}(q)$.

From a comparison of (3.8) and (3.5), we see that the difference between χ_{nn} and $\chi_{nn'}$, which is mainly represented by the term l/x in $\nu_{\pm}(l)$ of (3.8), becomes significant at the long wavelength limit ($x \to 0$). In other words, the inter-subband effect in the density response is most significant in the low q region. When $x \ll y - l$, (3.8) reduces to

$$\chi_{nn'}(q \to 0,\omega) = 2\frac{(k_{\mathrm{F}n} - k_{Fn'})/\pi}{\omega - (n'-n)\omega_0} + \mathrm{O}(q^2). \tag{3.11}$$

Equation (3.9) shows that in the $q \to 0$ limit, $\chi_{nn'}$ has a finite value, in contrast to $\chi_{nn}(q \to 0,\omega)$ which vanishes (see (3.7)). This $q \to 0$ lateral polarization is the source of the depolarization effect of the Q1D collective excitation, which we will further explore in section 5.2.

The basic features of the inter-subband polarizability matrix are illustrated by figure 2, where we plot the static function $-\chi_{01}(q)$ in units of $m^*/2\pi k_{\mathrm{F}}$, with $a = 0.01$ and 0.1, and $bk_{\mathrm{F}} = 1.73$ and 2.24. It can be seen from the figure that the static inter-subband matrix has a similar shape to that of $\chi_{nn}(q)$:

(i) it approaches a finite value as $q \to 0$;

(ii) it peaks at $q = k_{\mathrm{F}n} + k_{Fn'}$;

(iii) it vanishes as q^{-2} at $q \to \infty$.

The nature of the peak of $\chi_{nn'}(q)$ is similar to that of the intra-subband polarizability matrix $\chi_{nn'}(q)$, except for a down shift (for $n' > n$) of the peak position from $q = 2k_{\mathrm{F}n}$ for $\chi_{nn}(q)$ to $q = k_{\mathrm{F}n} + k_{Fn'}$ for $\chi_{nn'}(q)$. Also, both the peak value and width depends on the parameter a, and the peak becomes narrow when a decreases. In addition, the value of $-\chi_{01}(0)$ can be estimated from the general form deduced from (3.11) as

$$-\chi_{nn'}(q=0)/(m^*/2\pi k_{Fn}) = 4b^2 k_{\mathrm{F}n}(k_{\mathrm{F}n} - k_{Fn'})/(n'-n) \tag{3.12}$$

which is in contrast to the $q = 0$ value of the intra-subband polarizability matrix where we recall that

$$-\chi_{nn}(q=0)/(m^*/2\pi k_{\mathrm{F}n}) = 4.$$

For arbitrary nn', from (3.8*a*) we expect that $\chi_{nn'}(q)$ will keep the qualitative features of $\chi_{01}(q)$ as seen in figure 2.

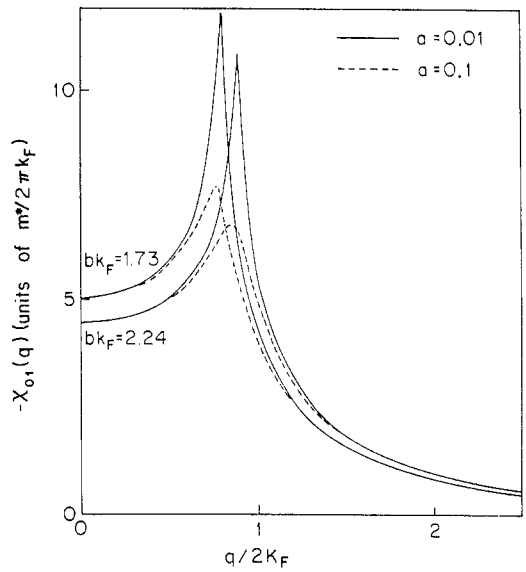

Figure 2. Static inter-subband polarization matrix elements $-\chi_{01}(q)$ (in units of $m^*/2\pi k_F$) as a function of $q/2k_F$ for $a = 0.01, 0.1$ and $bk_F = 1.73, 2.24$.

4. Dielectric matrix function

The dielectric response function of a Q1D system takes the form of a matrix. The generalized dielectric matrix function is given by [13,16]

$$\epsilon_{nn',mm'}(q,\omega) = \delta_{nm}\delta_{n'm'} - \chi_{nn'}(q,\omega)V_{nn',mm'}(q) \tag{4.1}$$

where the Coulomb matrix $V_{nn',nn'}(q)$ is defined by (2.4) and $\chi_{nn'}(q,\omega)$ is the polarization function. In the random phase approximation (RPA), the $\chi_{nn'}(q,\omega)$ in (4.1) is replaced by the non-interacting polarization matrix $\chi^0_{nn'}(q,\omega)$, i.e. (3.2) with $a \to 0$, and then (4.1) has the $q = 2k_F$ divergence problem. Here we go beyond the RPA by using the generalized polarization matrix (3.2), which includes the modifications to the response of the Q1D system due to the fluctuation effects.

First, we observe directly that the matrix elements in (4.1) can be regrouped into two decoupled (which we shall call the even and odd) blocks. The even block contains all those matrix elements with $n + n'$ and $m + m'$ as even numbers. In other words, the even block has all the M intra-subband terms as its diagonal part plus those inter-subband terms with even number separations for the related subbands, and the odd block has all the inter-subband terms with odd number separations for the related subbands. Also, the dimensionality of the even and odd blocks are the same except that when M is odd, the even block is one dimension larger than that of the odd block.

Next, we study the static dielectric matrix function $\epsilon_{nn',mm'}(q)$, the $\omega = 0$ expression of (4.1). Using (2.4) and (3.8a), from (4.1) we obtain

$$\epsilon_{nn',mm'}(q) = \delta_{nm}\delta_{n'm'} + \frac{1}{2\pi q a_B^*} E_{nn',mm'}(bq) \times \ln \frac{[(b_n - \nu_-(l))^2 + \frac{1}{4}a^2x^2][(b_{n'} + \nu_+(l))^2 + \frac{1}{4}a^2x^2]}{[(b_n + \nu_-(l))^2 + \frac{1}{4}a^2x^2][(b_{n'} - \nu_+(l))^2 + \frac{1}{4}a^2x^2]} \tag{4.2}$$

where $a_B^* = \kappa\hbar/m^*e^2$, the value of which depends on the material. In this paper we analyse the GaAs system, and take the ratio $b/a_B^* = 3.0$ from the experimental data.

There are two kinds of the diagonal elements of (4.2), the intra-subband ($n = n' = m = m'$) and the inter-subband ($n = m, n' = m'$) cases. The intra-subband expression of (4.2) is

$$\epsilon_{nn}(q) = 1 + \frac{1}{\pi q a_B^*} E_{nn}(bq) \ln \frac{(2k_{Fn} + q)^2 + a^2q^2}{(2k_{Fn} - q)^2 + a^2q^2} \tag{4.3}$$

which is obtained directly from (4.2) by definition and nn denotes $\{nn, nn\}$. The intra-subband dielectric matrix function (4.3) has the following features:

(i) it diverges logarithmically at $q \to 0$ (due to the logarithmic divergence of the intra-subband Coulomb matrix at $q \to 0$ as can be observed from (2.4));

(ii) it tends to one at $q \to \infty$; and

(iii) it has a turning point at $q = 2k_F$, where the value of $\epsilon_{nn}^{-1}(q)$ changes dramatically.

These features are illustrated by figure 3(a), where the dependence of the fluctuation parameter a is studied, and figure 3(b), where the dependence on the subband indices is studied.

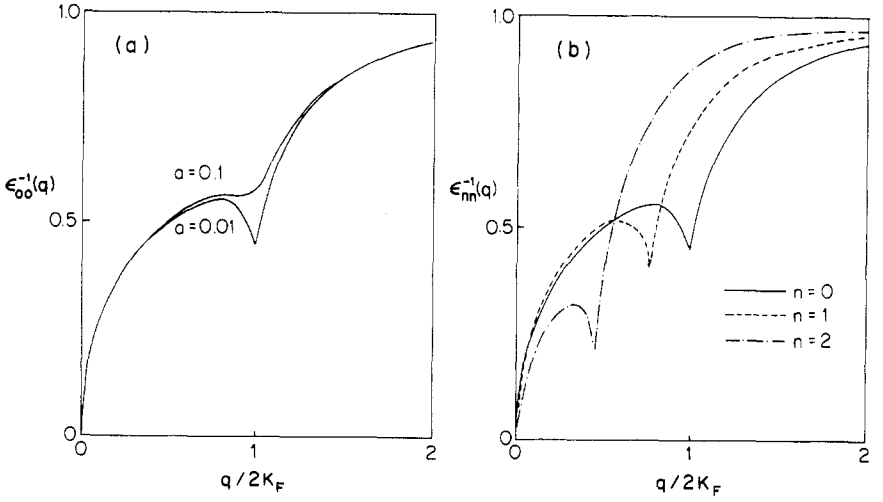

Figure 3. Inverse of the static intra-subband dielectric matrix function $\epsilon_{nn}(q)$ as a function of $q/2k_F$: (a) $n = 0$ for two broadening parameters $a = 0.1$ and 0.01; (b) $a = 0.01$ for three different subband indices $n = 0, 1, 2$.

The diagonal elements $\epsilon_{nn'}(q) \equiv \epsilon_{nn',nn'}(q)$ of the static inter-subband dielectric matrix (4.2), can be worked out correspondingly from (4.2). From (2.4) and (3.10a), it is easy to see that

$$\epsilon_{nn'}(q) = \epsilon_{n'n}(q). \tag{4.4}$$

Thus we have to study only one of the $\epsilon_{nn'}(q)$ and $\epsilon_{n'n}(q)$. In figure 4, we plot $\epsilon_{01}^{-1}(q)$ at $a = 0.01$, and 0.1 and $bk_F = 1.73$ and 2.24. Also, from (2.4), (3.12) and (4.1), we obtain the $q = 0$ value of the diagonal inter-subband dielectric matrix

$$\epsilon_{nn',nn'} = 1 + E_{nn',nn'}(q \to 0)\frac{2b^2}{\pi a_B^*}\frac{k_{Fn} - k_{Fn'}}{n' - n}. \tag{4.5}$$

Using the fact $E_{01,01}(q = 0) = 1$, we have $\epsilon_{01} = 1 + 2b^2(k_F - k_{F1})/\pi a_B^*$.

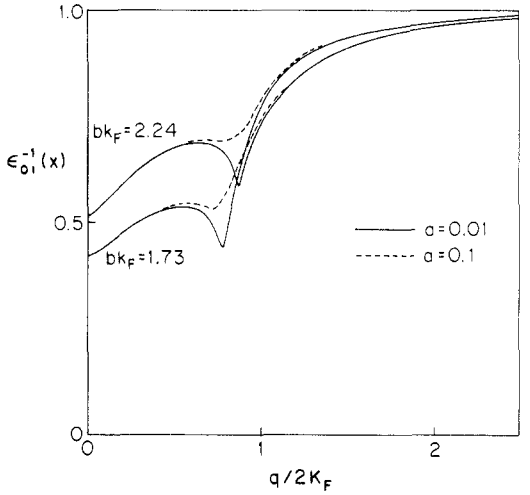

Figure 4. Inverse of the static inter-subband dielectric matrix function $\epsilon_{01}(q)$ as a function of $x = q/2k_F$ for $a = 0.01, 0.1$ and $bk_F = 1.73, 2.24$.

5. Applications

In this section we apply the formalism developed in the previous sections, the generalized Q1D polarizability, the analytic form of the Q1D Coulomb matrix elements, and the dielectric matrix elements, to study two of the most fundamental static and dynamic dielectric response phenomena, i.e. the impurity screening and plasmon excitations for the Q1D electron system.

5.1. Impurity screening

In the study of the multi-subband transport of a two-dimensional electron gas, a formal theory for the screened impurity potential has been developed [16], which involves the evaluation of the inverse of the dielectric matrix function. Due to the complexity of

the dielectric matrix, the actual evaluation of the screened potential has never been carried out explicitly. On the other hand, it is clear to see that the formal theory of the screened impurity potential of the multi-subband two-dimensional system is also applicable to the Q1D system. Here we apply the relatively simple form of the Q1D dielectric matrix function obtained in the previous sections to calculate explicitly the screened potential by means of the existing formal theory.

We start from the formula for the Fourier transform of the screened impurity potential [16]

$$U^{s}_{ij}(q) = \sum_{lm} [\epsilon^{-1}(q)]_{ij,lm} U_{lm}(q) \tag{5.1}$$

where $\epsilon^{-1}(q)$ is the inverse of the dielectric matrix function (4.1), and $U_{lm}(q)$ is the one-dimensional Fourier transform of the matrix element of the unscreened impurity potential, given explicitly by (with x and y now denoting the Cartesian coordinates)

$$U_{lm}(q) = \frac{2Ze^2}{\kappa} \int \mathrm{d}y\, \xi^{*}_{l}(y) K_0(qy) \xi_m(y) \tag{5.2}$$

where Z is the number of charges of the impurity and κ, K_0 and ξ_l are the same as in (2.4). Similar to (2.4), equation (5.2) can be evaluated analytically. For the present purpose, we give the results of (5.2) for the two subband case

$$U_{00}(q) = \frac{Ze^2}{\kappa} \mathrm{e}^{b^2q^2/8} K_0(\tfrac{1}{8}b^2q^2) \tag{5.3a}$$

$$U_{11}(q) = \frac{Ze^2}{\kappa} \mathrm{e}^{b^2q^2/8} \{K_0(\tfrac{1}{8}b^2q^2) + \tfrac{1}{4}b^2q^2[K_0(\tfrac{1}{8}b^2q^2) - K_1(\tfrac{1}{8}b^2q^2)]\} \tag{5.3b}$$

$$U_{01}(q) = U_{10}(q) = 0. \tag{5.3c}$$

We note that (5.3c) is true for any $U_{lm}(q)$ with $(l + m)$ an odd number. Recalling our earlier comments that the matrix $\epsilon(q)$ is decoupled into even and odd blocks, the vanishing of $U_{lm}(q)$ when $(l + m)$ is an odd number implies that only the even block of the matrix $\epsilon(q)$ contributes to the screened potential (5.1). From (5.1), it is straightforward to obtain the total screened-impurity potential

$$U^{s}(r_0) = \sum_{i} U^{s}_{ii}(r_0) = \frac{Ze^2k_F}{\kappa} \sum_{i} I_{ii}(r_0) \tag{5.4a}$$

with

$$I_{ii}(r_0) = \frac{2}{\pi} \int_0^{\infty} \mathrm{d}x_0\, \cos(x_0r_0) \sum_{lm} [\epsilon^{-1}(x_0)]_{ii,lm} U_{lm}(x_0)/(e^2/\kappa) \tag{5.4b}$$

where $x_0 = q/2k_F$, $r_0 = 2k_Fx$ and $(l + m)$ are even numbers. In the following, we evaluate (5.4) for a Q1D system having a total of two subbands with one or two populated subbands.

When the system is populated with electrons in a single subband, there is only one term in (5.4), i.e.

$$I_{00}(r_0) = \frac{2}{\pi} \int_0^{\infty} \mathrm{d}x_0\, \cos(x_0r_0) \epsilon^{-1}_{00}(x_0) U_{00}(x_0)/(e^2/\kappa). \tag{5.5}$$

We recall that for the high (two- and three-) dimensional systems, the screened potential has similar expressions to (5.5), with the replacement of dx_0, U_{00} and ϵ_{00} by their counterparts defined in higher dimensions. There, the screened potential diverges at $r_0 = 0$, and has the Friedel oscillation behaviour at large r_0 with $U^s_{00}(r_0 \to \infty) \sim \sin r_0/r_0^d$, $d = 2, 3$ for two and three dimensions. Equation (5.5) is different from the higher dimension screened potential in the following sense. First, at large r_0 one obtains from (4.3) and (5.5)

$$U^s_{00}(r_0) \sim \frac{1}{r_0} \sin\left(\frac{r_0}{1+a^2}\right) \tag{5.6}$$

which is a Friedel oscillation decaying much slower than in the higher dimensional case. Secondly, (5.5) is practically finite at $r_0 = 0$. This is because the integral in (5.5) is one-dimensional, and the integrand in (5.5) equals $\frac{1}{2}\pi k_F a_B^*$ at $q \to 0$ and goes as q^{-1} at $q \to \infty$, which are easily deduced from (5.3a) and (4.3). Thus, the screened potential (5.5) is a well defined quantity and has strong Friedel oscillation behaviour. In figure 5, we plot the screened potential (5.5) at $b/a_B^* = 3.0$, $a = 0.01$ and two different k_F values of $bk_F = 1.00$ and 1.34, where prominent Friedel oscillation is clearly demonstrated. We observe from the inset figure in figure 5 that when the fluctuation effect (represented by the parameter a) increases, the period of the Friedel oscillation increases and the amplitude decreases, which is similar to what was found in two-dimensional and three-dimensional systems. We note that the dependence on a of the screened potential (5.5) is weaker than that of the screened density, as only the denominator ϵ_{00} in (5.5) has a dependence on a at a relatively large value of $q/2k_F$.

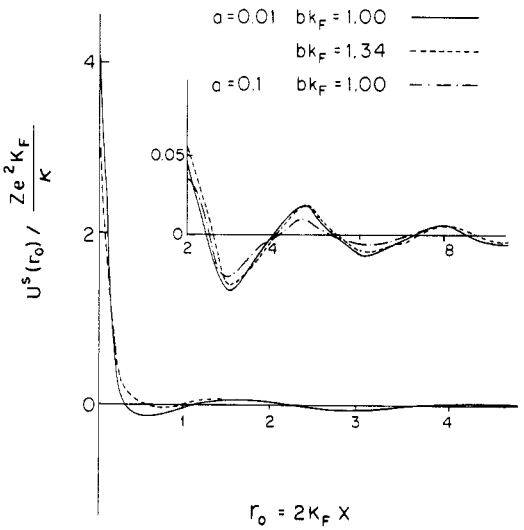

Figure 5. Screened impurity potential $U^s(r_0)$ (in units of Ze^2k_F/κ) against r_0 for a one subband Q1D system for different values of the fluctuation parameter a and Fermi momentum k_F.

When the two subband system is populated for both subbands, there are two terms in (5.4a), which is

$$U^s(r_0) = \frac{Ze^2k_F}{\kappa}[I_{00}(r_0) + I_{11}(r_0)] \tag{5.7}$$

where

$$I_{00}(r_0) = \frac{2\kappa}{\pi e^2}\int_0^\infty dx_0\, \cos(x_0 r_0)\{\epsilon_{1111}(x_0)U_{00}(x_0) - \epsilon_{0011}(x_0)U_{11}(x_0)\}/D_e(x_0) \tag{5.7a}$$

$$I_{11}(r_0) = \frac{2\kappa}{\pi e^2}\int_0^\infty dx_0\, \cos(x_0 r_0)\{\epsilon_{0000}(x_0)U_{00}(x_0) - \epsilon_{1100}(x_0)U_{11}(x_0)\}/D_e(x_0). \tag{5.7b}$$

Here

$$D_e(x_0) = \epsilon_{0000}(x_0)\epsilon_{1111}(x_0) - \epsilon_{0011}(x_0)\epsilon_{1100}(x_0) \tag{5.8}$$

and the $\epsilon_{ij,lm}(x_0)$ are defined by (4.2). In figure 6, we plot the numerical results of (5.7) at $b/a_B^* = 3.0$, $a = 0.01$ and two k_F values of $bk_F = 1.48$ and 1.95. The figure shows that the screened potential of a populated two subband system keeps the basic properties of a single populated subband system: the $U^s(r_0 = 0)$ is finite and the Friedel oscillation at large r_0 is relatively strong.

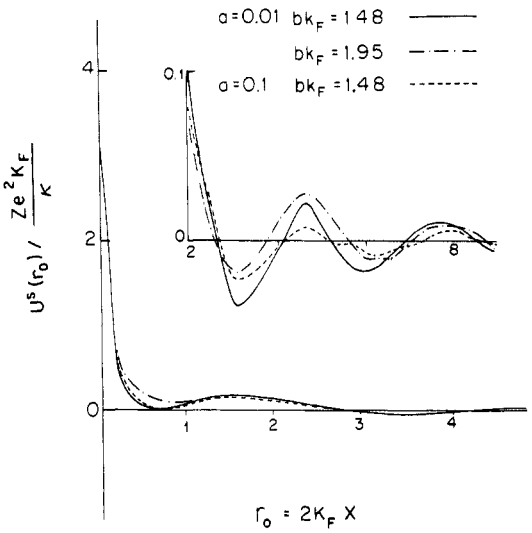

Figure 6. Screened impurity potential $U^s(r_0)$ (in units of Ze^2k_F/κ) against r_0 for a two subband Q1D system for different values of the fluctuation parameter a and Fermi momentum k_F.

When M is larger than two, the evaluation of (5.4) is much more tedious than the $M = 2$ case. This is because:

(i) the calculation of $\epsilon^{-1}(x)$ is more complicated; and

(ii) the non-vanishing off-diagonal term $U_{lm}(q)$ appears in (5.4*b*).

Nevertheless, in principle, the evaluation of the screened potential (5.4) in our formalism can be carried out for the Q1D system with arbitrary number of subbands.

6. Inter-subband plasmon excitation

The plasmon spectrum for a Q1D system is determined by the condition

$$\det(\epsilon_{ij,lm}) = 0 \qquad i,j,l,m = 0,1,2,\ldots,M-1 \tag{5.9}$$

which has a dimension of $M^2 \times M^2$. It is well known that for the ordinary plasmon in the low dimensional case, electrons in the same energy band (intra-band) oscillate collectively with a frequency $\omega \sim q^{1/2}$, $q|\ln q|^{1/2}$ respectively for two-dimensional and one-dimensional in the long wavelength limit. In a Q1D system many subbands are populated. As a result, the inter-subband plasmon for electron densities appears. Previously [13], we have used the Coulomb matrix (2.4) and the free electron polarizability (3.6), to solve (5.9). Our main conclusions concerning the spectrum of the inter-subband plasmon with a single subband separation are:

(i) it is relevant only to the odd sub-block of the dielectric matrix (4.1);

(ii) there are M different modes composing the collective excitations of a system with M populated modes; and

(iii) the maximum frequency ω_p^M of these M modes is proportional to the subband separation ω_0 and is determined by the largest value of the differences between the Fermi momenta of the electrons in the consecutive subbands.

Explicitly, when the top subband is significantly populated, it has the value [13]

$$\omega_p^M = \omega_0 \left(1 + \frac{4}{\pi}\frac{b^2 k_{F,M-1}}{a_B^*}\right)^{1/2} \tag{5.10}$$

where $k_{F,M-1}$ is defined in (3.3). However, $k_{F,M-1}$ is replaced by $k_{F,M-2} - k_{F,M-1}$ when the top subband is almost empty. Here we use (5.10) to discuss the relationship between the inter-subband plasmon frequency and the electron density, which is motivated by the following unexplained experimental results. In their experiments [1,2], Hansen *et al* found that when the electron density decreases the inter-subband plasmon frequency increases. Their result is displayed by figure 7, where we are concerned only with the Q1D behaviour, the left part of the figure. That collective effects are most important at the lowest electron density seems surprising. Because such collective effects, which in the simplest approximation are associated with classical depolarization, are naively expected to become less important with decreasing electron density and to vanish as $\omega_p \sim n_s^{1/2}$. This remains unexplained in the recent theoretical studies using the 'few subband approximation' [8,9]. On the other hand, our result (5.10) does not have the restriction of few subbands and the density dependence of ω_p^M can be easily calculated once the quantities appeared in (5.10) are given. Using the data given or extracted from table 1 of [2], for ω_0, b, a_B^*, and k_{FM} at three different densities $N_{1D} = 6.7, 6.1, 3.7 (10^6\ \mathrm{cm}^{-1})$ (corresponding to the gate voltage $V_g = -500, -550, -600$ (mV) in figure 7), we have evaluated ω_p^M of (5.10) as a function of electron density. The result is presented in figure 7 by open circles. As can be seen from the figure, our theoretical results are very consistent with the experimental data: when the Fermi energy decreases (so does the electron density) the inter-subband plasmon frequency increases. According to (5.10), the inter-subband plasmon ω_p^M frequency depends on the subband separation ω_0 and the maximum value of the differences between the Fermi momentum of the consecutive subbands,

the larger the ω_0 and the $k_{F,M-1}$, the larger ω_p^M will be. When the magnitude of the gate voltage of the Q1D system increases (as in the experiments of [1, 2]), the strength of the harmonic confinement potential increases, and an increase of subband separation ω_0 follows. At the same time, if ω_0 becomes larger, electrons in the top subband can have higher Fermi momentum than before since by definition the maximum value of k_{FM} equals $\sqrt{2m^*\omega_0}/\hbar$. It is the combined effect of the increase of ω_0 and k_{FM} at the decreasing gate voltage that determines the increasing of the ω_p^M, which explains the experimental finding of [1, 2].

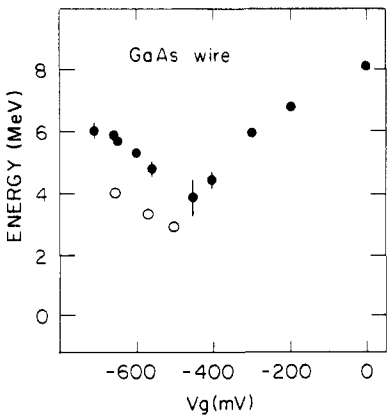

Figure 7. Resonance energies of the infrared excitations: A comparison between the theoretical results of $\hbar\omega_p^M$ (ω_p^M is the inter-subband plasmon frequency) as obtained by (5.10) (open circle) and the experimental data (dots) of [2] V_g is the gate voltage. The parameters used in the calculation are obtained from table I of [2].

Finally we note that the quantitative agreement between the theoretical values and the experimental results as seen in figure 7 can be improved if we consider:

(i) the interactions between the inter-subband plasma;

(ii) finite q contributions to (5.10); and

(iii) slightly larger values of ω_0 than the experimentally given values.

7. Summary

In this paper, we have studied the dielectric response of a Q1D electron system in the harmonic confinement potential model.

The generalized Q1D polarizability (2.7) is derived by extending the generalization of the Lindhard function to include the fluctuation. At $T = 0$, we obtain analytical expressions for the intra- and inter-subband polarizability matrix element (3.5) and (3.8), respectively. Equations (2.7), (3.5) and (3.8) rigorously obey the charge neutrality requirement of the density response function, and are free of the divergence problem originally present in the free electron polarizability. Detailed study of the static function shows that the intra-subband polarizability (3.5) has a q dependence similar to that of the two-dimensional and three-dimensional polarizabilities, while the inter-subband polarizability (3.8) obeys the symmetry properties (3.9) and (3.10). The inter-subband effect in the polarizability is found to be most significant in the

low q region. In particular, $\chi_{nn'}(q \to 0, \omega)$ has a finite value of (3.11) in contrast to $\chi_{nn}(q \to 0, \omega)$ which vanishes.

By using a recently derived analytical form (2.4) of the electron–electron interactions of Q1D system in the harmonic confinement potential model, we obtain the analytic Q1D dielectric matrix function (4.2). The dependence of the fluctuation parameter a and the electron density (through the Fermi momentum) of the dielectric matrix function both for the intra- and inter-subband cases have been studied. Again, the $q = 0$ value of the inter-subband dielectric matrix function has a finite value in contrast to that of the intra-subband case where the dielectric matrix function diverges. Also, the dielectric matrix in the harmonic confinement potential model is found to be decoupled into two uncorrelated subblocks, the even and odd block, containing different physics. The even block of the dielectric matrix determines the properties of the impurity screening, while the odd block is responsible for the inter-subband plasmon excitation with a single subband separation.

The Q1D dielectric response theory is applied to study impurity screening and the inter-subband excitations in the presence of multi-subbands. We have presented a general expression for the total screened impurity potential (5.4) of the Q1D system, and studied it explicitly for a two subband system with either one or both subbands populated. We found that the total screened-impurity potential at the origin is a well defined quantity in contrast to the two-dimensional and three-dimensional case where it diverges. In addition the Friedel oscillation at large r_0 is much stronger than for the two-dimensional and three-dimensional cases. This implies that the Friedel oscillation of Q1D electron system, compared to the two-dimensional and three-dimensional systems, should be more easily detectable by experiments. In applying our formalism to the study of the inter-subband plasmon, we find that the plasmon frequency depends on the subband separation and the maximum value of the differences between the Fermi momentum of the consecutive subands. When the subband separation increases due to the strengthening of the confinement potential, the Fermi momentum of the top populated subbands also increases. Thus, when the magnitude of the gate voltage is increased to strengthen the confinement potential as was done in the experiments of [1, 2], we find an increase in the inter-subband plasmon frequency. Our theoretical result (5.10) is in good agreement with the experimental data of [2].

Acknowledgments

The work was supported in part by the US Office of Naval Research under Grant No N00014-90-J-1124.

References

[1] Hansen W, Horst M, Kotthaus J P, Merkt U, Sikorski Ch and Plogg K 1987 *Phys. Rev. Lett.* **58** 2586
Kotthaus J P 1989 *Nanostructure Physics and Fabrication* ed M A Reed and W P Kirk (New York: Academic) p 67
[2] Brinkop F, Hansen W, Kotthaus J P and Ploog K 1988 *Phys. Rev.* B **37** 6547
[3] Friesen W I and Bergersen B 1980 *J. Phys. C: Solid State Phys.* **13** 6627
[4] Lee Y C, Ulloa S E, and Lee P S 1983 *J. Phys. C: Solid State Phys.* **16** L995
Mendoza B S and Lee Y C 1989 *Phys. Rev.* B **40** 12063
[5] Das Sarma S and Lai W Y 1985 *Phys. Rev.* B **32** 1401

[6] Lai W and Butcher P N 1988 *J. Phys. C: Solid State Phys.* **21** 4367
[7] Jain J K and Das Sarma S 1988 *Phys. Rev.* **36** 5949
[8] Que W and Kirczenow G 1988 *Phys. Rev.* **37** 7153
[9] Li Qiang and Das Sarma S 1989 *Phys. Rev.* B **40** 5860
[10] Mermin D 1970 *Phys. Rev.* B **1** 2362
[11] Hu G Y and O'Connell R F 1989 *Phys. Rev.* B **40** 3600
[12] Hu G Y and O'Connell R F 1988 *J. Phys. C: Solid State Phys.* **21** 4325
[13] Hu G Y and O'Connell R F 1990 *Phys. Rev.* B **42** 1290
[14] Efetov K B and Larkin A I 1976 *Sov. Phys.-JETP* **42** 390
Prigodin V N 1980 *Sov. Phys.-JETP* **51** 636
Suzumura Y and Fukuyama H 1983 *J. Phys. Soc. Japan* **52** 2870
Barisic S 1985 *Electronic Properties of Inorganic Quasi-One-Dimensional Compounds, Part I: Theoretical* ed P Monceau (Dordrecht: Reidel) pp 1–40
[15] Hu G Y and O'Connell R F 1987 *Phys. Rev.* B **36** 5798
[16] Ando T, Fowler A B, and Stern F 1982 *Rev. Mod. Phys.* **54** 437